Ari Laiho, Bernd M. Smarsly, Charl F. J. Faul, and Olli Ikkala. 2008. Macroscopically aligned ionic self-assembled perylene-surfactant complexes within a polymer matrix. Advanced Functional Materials, volume 18, number 13, pages 1890-1897.

FULL PAPER

ADVANCED FUNCTIONAL MATERIALS

DOI: 10.1002/adfm.200701496

Macroscopically Aligned Ionic Self-Assembled Perylene-Surfactant Complexes within a Polymer Matrix**

By *Ari Laiho, Bernd M. Smarsly, Charl F. J. Faul,** and *Olli Ikkala**

Ionic self-assembled (ISA) surfactant complexes present a facile concept for self-assembly of various functional materials. However, no general scheme has been shown to allow their overall alignment beyond local polydomain-like order. Here we demonstrate that ionic complexes forming a columnar liquid-crystalline phase in bulk can be aligned within polymer blends upon shearing, taken that the matrix polymers have sufficiently high molecular weight. We use an ISA complex of *N*,*N*′-bis(ethylenetrimethylammonium)perylenediimide/bis(2-ethylhexyl) phosphate (Pery-BEHP) blended with different molecular weight polystyrenes (PS). Based on X-ray scattering studies and transmission electron microscopy the pure Pery-BEHP complex was found to form a two-dimensional oblique columnar phase where the perylene units stack within the columns. Blending the complex with PS lead to high aspect ratio Pery-BEHP aggregates with lateral dimension in the mesoscale, having internal columnar liquid-crystalline order similar to the pure Pery-BEHP complex. When the Pery-BEHP/PS blend was subjected to a shear flow field, the alignment of perylenes can be achieved but requires sufficiently high molecular weight of the polystyrene matrix. The concept also suggests a simple route for macroscopically aligned nanocomposites with conjugated columnar liquid-crystalline functional additives.

1. Introduction

Self-assembly[1–8] allows preparation of nanostructured matter but, as such, typically leads only to local domain-like structures and therefore poor macroscopic order. Therefore, there have been extensive efforts to find simple and practical ways to extend and to align such local structures to macroscopic length scales.[8–16] Therein the aim is to promote functionalities and to achieve macroscopically anisotropic materials and properties. One general approach for self-assembly involves surfactant-based supramolecular complexes.[5,6,17] Although high overall alignment has been achieved in the case of hydrogen-bonded self-assembled polymer-amphiphile systems,[11,18,19] the alignment of ionic self-assembled (ISA) complexes between charged materials and oppositely charged surfactants has remained far more challenging. Solving this is of scientific and practical importance, as the strength of ionic interaction would suppress the tendency of the macroscopic phase separation between the surfactant and the backbone, which is important, e.g., for conjugated electroactive materials with a strong aggregation tendency. Also, ISA complexes are versatile materials that allow facile combination of various functionalities in a modular fashion by complexing different charged functional moieties with ionic surfactants. The surfactants not only allow tuning of the assembly and packing and introduce plasticization, but can also lead to liquid crystallinity.[5]

Perylenes are important organic electron-accepting semiconducting moieties.[20] Ionic complexes between perylenes functionalized by charged groups and oppositely charged surfactants have been demonstrated.[21,22] Even if it is straightforward to achieve self-assembled local structures therein, it is surprisingly difficult to achieve common macroscopic alignment beyond the local order. In fact, this drawback is a common property for ISA materials.[16] A potential reason is the high density of charges, leading to strong and long-range Coulomb interactions with reduced relaxations and to the high viscosity. Classical alignment strategies, such as shear alignment,[23] electric and magnetic fields, or rubbing with pre-treated surfaces (PTFE or polyimides) showed negligible alignment of ionic self-assembled materials.[22] Only recently[16,24] has it been shown that, by incorporating photoactive units, photo-orientation can

[*] Dr. C. F. J. Faul
School of Chemistry, University of Bristol
Bristol BS8 1TS (UK)
E-mail: charl.faul@bristol.ac.uk
Prof. Dr. O. Ikkala, A. Laiho
Department of Engineering Physics
and Center for New Materials
Helsinki University of Technology
P.O. Box 5100, 02015 TKK, Espoo (Finland)
E-mail: olli.ikkala@tkk.fi
Prof. B. Smarsly
Physikalisch-Chemisches Institut
Justus Liebig Universität Gießen
Heinrich Buff Ring 58, 35392 Gießen (Germany)

[**] We thank Dr. Laszlo Almasy (Helsinki University of Technology) for useful discussions. This work has been supported as part of the European Science Foundation Collaborative Research (EUROCORES) Programme on Self-Organised NanoStructures (SONS). The University of Bristol, MPG and the Academy of Finland are acknowledged. The work was partly carried out in the Centre of Excellence of Finnish Academy (Bio- and Nanopolymers Research Group, 77317). C.F.J.F. thanks HUT for a visiting professorship.

ADVANCED FUNCTIONAL MATERIALS

lead to aligned nanostructures. However, this strategy would not be generally applicable due to the required inclusion of such photo-active units.

Shear flow is intrinsically present in several processes and could be a practically important alignment concept. However, shearing as such leads to hardly any degree of alignment of ISA-complexes.[23] Specifically, this approach has been tried on ISA complexes of perylenediimides with little success in our laboratories. Nevertheless, the alignment of the n-type conducting perylene moieties is especially desirable, as perylene derivatives are attractive for supramolecular materials,[20] photovoltaics,[25] molecular electronics,[26] liquid-crystalline materials[21,22,27] and optical components.[22]

Here we therefore introduce a concept that enables an overall alignment strategy for ionic self-assembled complexes, i.e., by blending ISA complexes in a high molecular weight commodity polymer matrix, such as polystyrene (PS), and thereafter shearing the blend. Here we use the cationic *N*,*N*′-bis(ethylenetrimethylammonium)-perylenediimide (Pery) ionically self-assembled with anionic bis(2-ethylhexyl) phosphate (BEHP) surfactants (for the chemical formulas, see Fig. 1a). Not only would such materials contain functional perylene moieties, but, based on related complexes studied previously, can well-defined self-assembled stacked structures be expected in this case.[21,22]

Although this approach seems rather logical, and closely analogous to various current investigations into blending of clay platelets[28] or even carbon nanotubes[29] with commodity polymers, the concept seems to have been largely overlooked for self-assembled materials, and could be of great practical value. The previous literature describes how, e.g., smectic liquid crystal,[30] electrically conducting[31–33] or semiconducting polymers,[34,35] and porogens[36,37] have been blended within matrices. However, possibilities to achieve anisotropic properties have been less studied. Still another approach is based on self-assembling dendronized rod-coil (DRC) systems[38] as an organogelator at very low concentrations in organic monomeric solvents, such as styrene and acrylates.[39] When such gelled monomer and DRC mixtures were polymerized, the DRC self-assembled scaffold was still present, with the resulting (normally amorphous) polymers exhibiting birefringence, enhanced mechanical properties and enhanced chain orientation after drawing from melts.[39,40]

2. Results and Discussion

2.1. Structure of Self-Assembled Pery-BEHP

As a background, the self-assembled structure of the pure Pery-BEHP complex (Fig. 1a) is first assessed using wide- and small-angle X-ray scattering (WAXS and SAXS) as well as transmission electron microscopy (TEM). From WAXS measurements the perylene units are observed to stack with a d-spacing of 3.4 Å, characteristic for π-stacking (see the inset of Fig. 1b, which shows the reflection at a scattering angle of $2\theta = 26.2^\circ$). SAXS indicates a well-ordered structure with several distinct reflections (Fig. 1b). The scattering pattern can be indexed[41] to a two-dimensional oblique columnar phase with a unit cell $a = 39.8$ Å, $b = 23.9$ Å and $\gamma = 62.0^\circ$ (Fig. 1d). The two-dimensional columnar structure is also revealed by the TEM micrographs (Fig. 1c), which show a long period of approximately 23 Å, in close agreement with the 110 reflection of the complex ($d_{110} = 2\pi/q_{110} \approx 23.8$ Å).

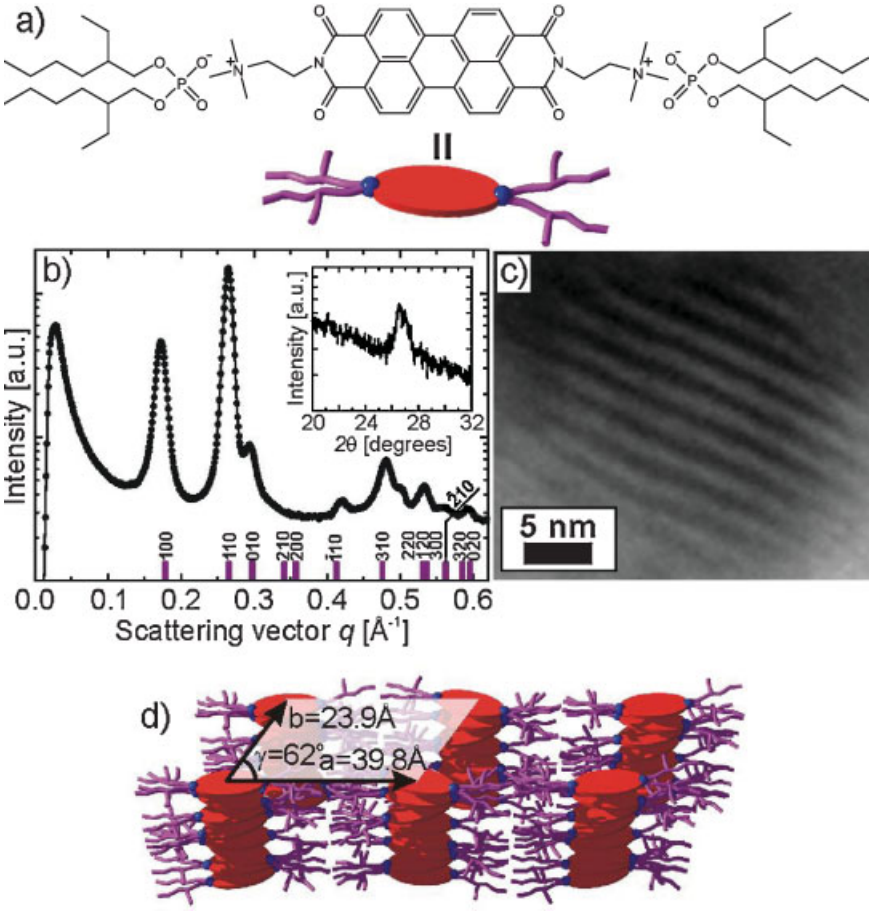

Figure 1. Ionic self-assembled *N*,*N*′-bis(ethylenetrimethylammonium)-perylenediimide/bis(2-ethylhexyl) phosphate complex, i.e., Pery-BEHP. a) The chemical formula and schematic representation illustrating the planar perylene unit capable of π-stacking and the plasticizing surfactant tails. b) SAXS intensity pattern, where the positions of the reflections for the fitted structure are indicated ($a = 39.8$ Å, $b = 23.9$ Å, $\gamma = 62^\circ$). The inset shows the WAXS reflection for scattering angles characteristic for the π-stacking. c) TEM micrograph. d) Scheme of the proposed oblique columnar structure.

However, even if SAXS and TEM indicate well-defined order at the mesoscale, pure Pery-BEHP is isotropic on the macroscopic length scale and shows a polydomain structure. This is shown by the 2D SAXS pattern where isotropic Debye rings are observed (from which the pattern of Fig. 1b was, in fact, radially averaged). Therefore, the observed domains show internal columnar self-assembled structures, but lack common mutual alignment. In an effort to align the local columnar structures or, even more preferably, in order to achieve monodomain structure, samples of the pure ISA complex were subjected to oscillatory or steady shear flow using a stress-controlled rheometer. A wide variety of different temperatures and rheological conditions were used. However, no significant macroscopic alignment was achieved as revealed by SAXS. This did not come as a surprise, as this has been the general experience with other ISA complexes and underlined the fact that it is difficult to align the ISA-complexes by flow or other means.[16] As suggested before, the presence of the large number of charges in the ionic complexes may strongly suppress the structural reorganizations (required during the alignment process) due to the strong long-range Coulomb interactions. This interpretation is also supported by the high viscosity of the Pery-BEHP complex (see Fig. 2, to be discussed in more detail later). Still, keeping the large application potential of the ionic complexes in liquid crystals, photonic, and electroactive materials in mind, the problem to align the local self-assembled structures constituted a challenge that could not be ignored.

Therefore, the main motivation of this work was the following: the ''dilution'' of charges of the ionic complexes through the addition of nonpolar material could promote structural reorganizations during shear and could open practical routes towards overall alignment of the self-assembled structures. However, even if structural reorganizations were promoted, the functionality provided by the ionic complex is also diluted, which thus requires a careful balancing between these two competing factors. Within the present concept, the branched alkyl tails of the surfactant component, BEHP, are of particular relevance. First, being amorphous and mobile, they efficiently plasticize the complex but still allow the perylene units to pack to exhibit columnar liquid crystallinity, as shown in Figure 1d. The ethyl hexyl tails are also surface active towards nonpolar polymers, thus reducing the tendency for complete macroscopic phase separation in blends and allow preparation of nanocomposites.

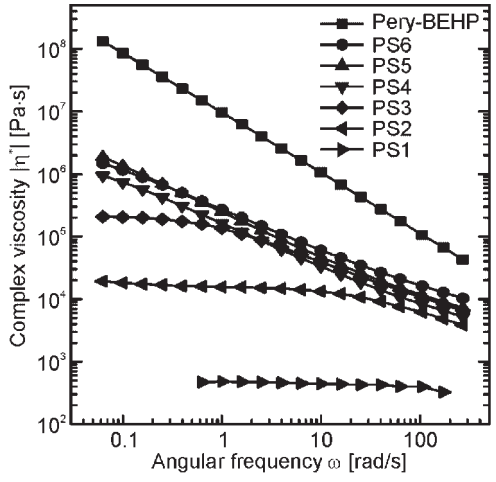

Figure 2. Complex viscosity of pure Pery-BEHP and six different pure PS samples at 150 °C, where the molecular weights of PS range from 6 000 g mol^{-1} (PS1) to 302 900 g mol^{-1} (PS6). See Table 1 for the molecular weights and details.

2.2. Blends of Pery-BEHP with PS

Pery-BEHP/PS blends were prepared by chloroform casting using several Pery-BEHP concentrations versus the total compositions, i.e., 0.01, 0.1, 1, 5, 10 wt % (for compactness and clarity only the 5 wt % composition is considered here). During polarized optical microscopy investigation of the prepared samples no macroscopic phase separation between Pery-BEHP and PS was observed, indicating surface activity of the ethyl hexyl tails towards PS. On the other hand, Figure 3b shows the SAXS reflections of the 5 wt % Pery-BEHP/PS blend using PS with $M_n = 115\,000$ g mol^{-1}. Two Debye rings are observed at $q = 0.16$ and 0.26 Å^{-1} (see Fig. 3b), which correspond to the 100 and 110 reflections of pure Pery-BEHP. This indicates that, even though no macroscale phase separation is observed, molecular level miscibility is not achieved either. Pery-BEHP must be dispersed in the PS matrix so that at least some of the dimensions of the aggregates are mesoscale, i.e., smaller than macroscopic. We expected the relative viscosities of Pery-BEHP and PS to play an important role in the shearing, as suggested by classic polymer blends.[42,43] Therein an extended dispersion or even phase continuity without droplet break-up could be obtained for the minority phase if the viscosity of the matrix component is selected to be sufficiently high. However, the present case can be much more subtle because of the stabilization due to surface activity between the two phases.

Encouraged by these considerations, we selected a series of PS homopolymers with different molecular weights ranging from 6 000 g mol^{-1} to 302 900 g mol^{-1}, with narrow polydispersities in the range 1.03–1.09 (Table 1). The viscosities of the homopolymers and pure Pery-BEHP, as determined at 150 °C using oscillatory shear flow, cover a wide range (Fig. 2). The temperature was selected to be as high as possible to promote the flow of the Pery-BEHP complex but still well below the degradation temperatures of both the complex and the polymers. Still, the pure Pery-BEHP complex exhibits high viscosity throughout the dynamic range, which also manifests as difficulty in processing. The three lowest molecular weight (MW) polymers show a Newtonian plateau in complex viscosity for the used rheometer. For the highest MW polymers and the pure Pery-BEHP complex such a plateau was not observable at 150 °C due to limitations in the maximum available torque of the rheometer.

ADVANCED FUNCTIONAL MATERIALS

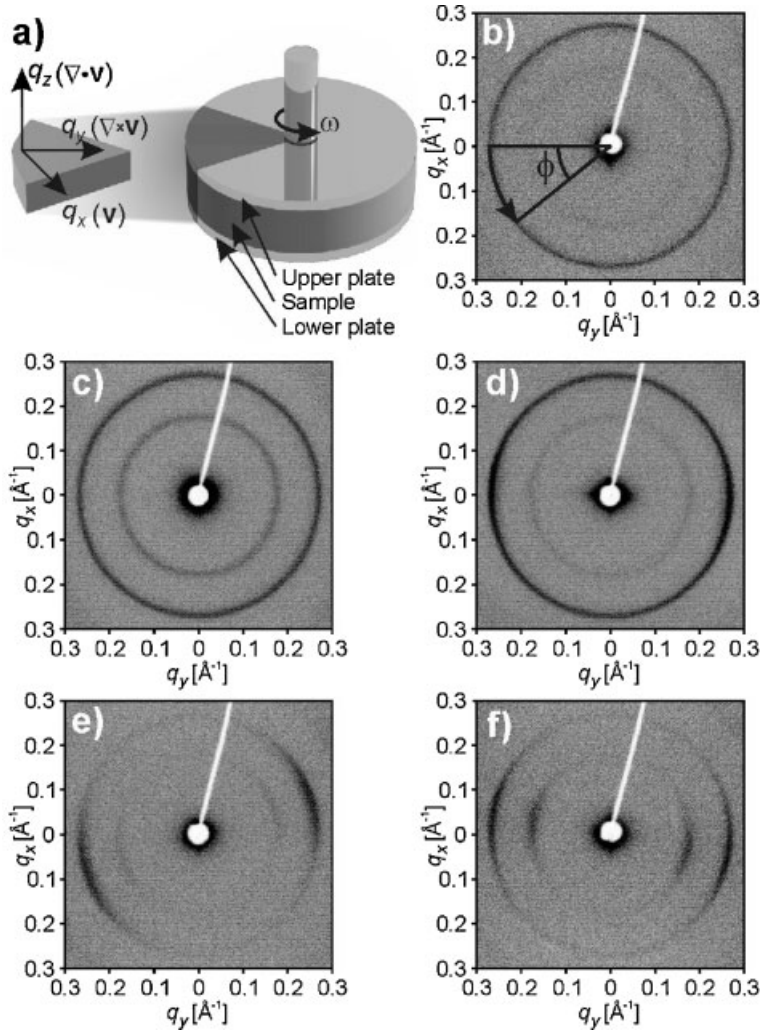

Figure 3. a) Scheme of the plate/plate geometry where the lower plate is fixed and the upper plate is rotated to produce shear flow to the sample between the parallel plates. The sample slice shows the corresponding coordinate axes where q_x is the direction of the flow field (**v**) and q_z shows the direction of the incident X-ray beam. SAXS intensity patterns for b) Pery-BEHP/PS4 sample prior to shear alignment showing also the azimuthal angle ϕ and SAXS intensity patterns for shear aligned c) Pery-BEHP/PS1, d) Pery-BEHP/PS2, e) Pery-BEHP/PS3, f) Pery-BEHP/PS4.

2.3. Shear Alignment of Pery-BEHP/PS Blends

In order to align the Pery-BEHP/PS blends, the sample pellets (50 μm in thickness and 10 mm in diameter) were heated to 150 °C and were subjected to steady shear flow of $\dot{\gamma}(t) = v(t)/h = 100\ s^{-1}$, where $v(t)$ is the velocity of the rheometer plate at half radius and h is the thickness of the sample. After shear alignment the sample pellets were allowed to cool to room temperature at ≈5 °C min^{-1}. The aim was to impose shear flow for 10 s on all Pery-BEHP/polymer blends. This was realized for the lower MW blends Pery-BEHP/PS1–Pery-BEHP/ PS4, whereas the highest MW blends (Pery-BEHP/PS5 and Pery-BEHP/PS6, see Table 1) were difficult to shear due to their high viscosity at 150 °C. Thus, in the latter two cases, the desired shear flow conditions could typically only be employed for 3–4 s before the rheometer was unable to provide high enough torque. As the high shear stress could not be maintained due to these device limitations, these two samples are therefore not considered in further discussions.

Prior to shearing, no macroscopic alignment is observed in any of the blends. This is illustrated in the SAXS pattern of the Pery-BEHP/PS4 blend containing 5 wt % of Pery-BEHP (Fig. 3b). Upon shearing, the 5 wt % blend with the lowest MW PS, i.e., PS1, shows hardly any alignment, as evidenced in Figure 3c. However, as the MW of the PS is increased, the alignment of the Pery-BEHP complex systematically improves (Fig. 3c–f). The results show that increasing the MW of the PS matrix within a certain window results in better alignment.

In order to quantify the degree of alignment, we determined a so-called orientation factor f_z for each aligned structure according to Hermans' method[44]

$$f_z = 1 - \frac{3}{2}\langle \sin^2 \varphi \rangle \quad (1)$$

where ϕ is the azimuthal angle in the intensity pattern (see Fig. 3b) and

$$\langle \sin^2 \varphi \rangle = \frac{\int_0^{\frac{\pi}{2}} I(\varphi) \sin^3 \varphi \mathrm{d}\varphi}{\int_0^{\frac{\pi}{2}} I(\varphi) \sin \varphi \mathrm{d}\varphi} \quad (2)$$

where $I(\phi)$ is the scattered intensity along the angle ϕ. The orientation factor $f_z = 1$ for perfectly oriented structure and $f_z = 0$

Table 1. Polystyrenes used.

Sample	M_n [g mol^{-1}]	M_w/M_n
PS1	6 000	1.06
PS2	24 000	1.03
PS3	50 000	1.04
PS4	115 000	1.04
PS5	202 000	1.05
PS6	302 900	1.09

for a randomly oriented (isotropic) structure. Orientation factors for the aligned samples were determined from the azimuthal intensity distribution $I(\phi)$ at $q = 0.26\,\text{Å}^{-1}$, which refers to the 110 reflection of the complex as listed in Table 2.

At present we are not able to give conclusive reason why increasing the MW of the matrix polymer promotes the alignment of Pery-BEHP, even if the result can be intuitively reasonable to accept. The values of the orientation factors f_z correlate with the number of entanglements within the matrix polymer. The entanglement molecular weight[45] of PS is roughly $M_e = 13\,000\,\text{g mol}^{-1}$, which means that the Pery-BEHP/PS4 sample (PS $M_n = 115\,000$) has on an average 9 entanglements per chain, whereas the lowest molecular weight sample Pery-BEHP/PS1 ($M_n = 6000\,\text{g mol}^{-1}$) has hardly any entanglements at all. In other words, when the higher molecular weight blends are subjected to steady shear flow, a long-range flow field is promoted due to the entanglements, which can also align the shape-persistent anisotropic mesoscale aggregates of Pery-BEHP. In the case of the lower molecular weight matrix polymers, the matrix merely acts as dispersing medium for the self-assembled domains and no essential alignment is observed upon imposing shear fields. This observation also suggests that simply diluting the columnar complexes in an organic solvent is not expected to lead to efficient alignment under shear.

Polarized UV-Vis spectroscopy was employed to provide further evidence of the alignment. First a scan of the polarization angle of the incident beam was performed at a constant wavelength on shear-aligned matrix blanks (i.e., pure PS samples containing no Pery-BEHP) and shear-aligned samples to minimize the errors in sample orientation (see Fig. 4). The dichroic ratios of the oriented samples were then determined by measuring the absorbance at two different angles in relation to the plane polarized light used for illumination, namely at perpendicular and parallel angles with respect to the flow direction (directions q_y and q_x, respectively, in Fig. 3a). By dividing the former absorbance value with the latter, the dichroic ratio at that particular wavelength is obtained. The dichroic ratios show a systematic increase as a function of the MW of the blended PS, as can be seen from Figure 5. This observation is also in full agreement with the structural analysis results obtained from SAXS. The highest value for dichroic ratio is obtained for the Pery-BEHP/PS4 (Fig. 5 curve e), ca. 1.48), which was also observed to possess the best shear alignment based on SAXS. The absolute values

Table 2. Values of the orientation factor f_z for shear aligned Pery-BEHP/PS samples determined from the intensity patterns shown in Figure 3. Before the alignment all of the blends showed small values in the range $f_z = 0.01$.

Sample	f_z
Pery-BEHP/PS1	0.04
Pery-BEHP/PS2	0.17
Pery-BEHP/PS3	0.48
Pery-BEHP/PS4	0.51

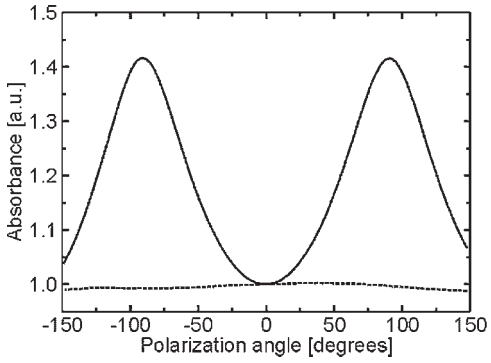

Figure 4. Polarization scan at $\lambda = 550$ nm on a shear-aligned Pery-BEHP/PS4 sample (solid line). The dashed curve shows a pure polystyrene blank matrix sample (PS4) that was subjected to similar shearing conditions as the PeryBEHP/PS4 sample. Zero angle is defined as the direction of the flow field.

for the dichroic ratio seem, at first, moderate when compared to values reported in literature.[16] However, one should bear in mind that in this investigation the contribution to the absorbance due to reflection, scattering and absorption originating from the polystyrene matrix alone has not been subtracted. Within the studied wavelength range this contribution remains constant as a function of the polarization angle of the incoming light (see Fig. 4). Had this contribution been subtracted from the absorbance values, the dichroic ratios would have been much higher. However, from a technological point of view, this subtraction could not be justified.

We obtained further evidence of the alignment direction of the perylenes from the polarization angle at which the absorbance is highest, namely perpendicular to the flow direction (see Fig. 4). Also, a further hint at the supramolecular structure and organization of the assembled mesogens comes from the shape of the UV-vis absorption spectra. If the shape of

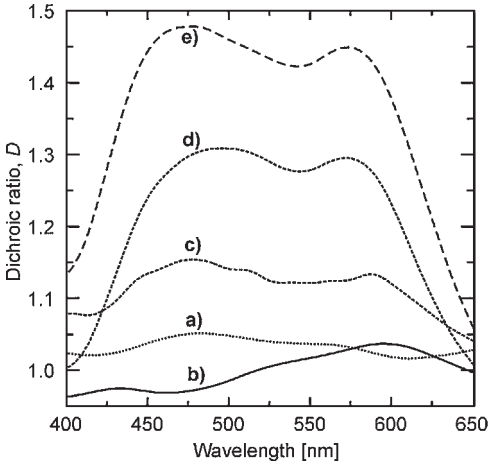

Figure 5. Dichroic ratio for a) Pery-BEHP/PS4 sample prior to shear alignment and for shear aligned b) Pery-BEHP/PS1, c) Pery-BEHP/PS2, d) Pery-BEHP/PS3, and e) Pery-BEHP/PS4, where the MW of PS increases from 6,000 g mol^{-1} (PS1) to 115 000 g mol^{-1} (PS4).

ADVANCED FUNCTIONAL MATERIALS

the full UV spectrum is compared with data gathered for Pery- AOT complexes,[22] the shapes are quantitatively the same. In the case of the Pery-AOT complexes it was found that the perylene dyes were arranged in columns (i.e., along the *x*-axis), with the dipole transition moments of the perylene dyes mostly isotropically distributed perpendicular to the columns in the yz plane (see Fig. 6 for a corresponding geometry).

The optical anisotropy of the shear aligned sample pellets can also be resolved with a polarizing microscope, where the polarizers are set in orthogonal directions (i.e, crossed) and the sample pellet is then placed between the polarizers. For example, the Pery-BEHP/PS4 exhibits a Maltese cross type pattern (see Fig. 7b) between crossed polarizers, indicative of a uniform alignment throughout the sample pellet.

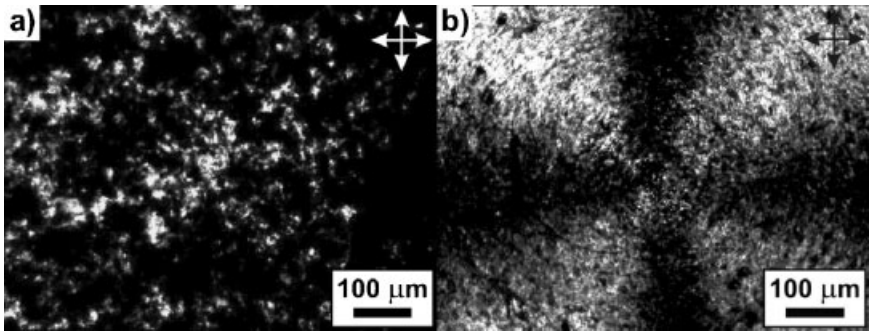

Figure 7. Polarized optical micrographs of the Pery-BEHP/PS4 sample a) before and b) after shear alignment. Observe the Maltese cross type pattern due to shear alignment.

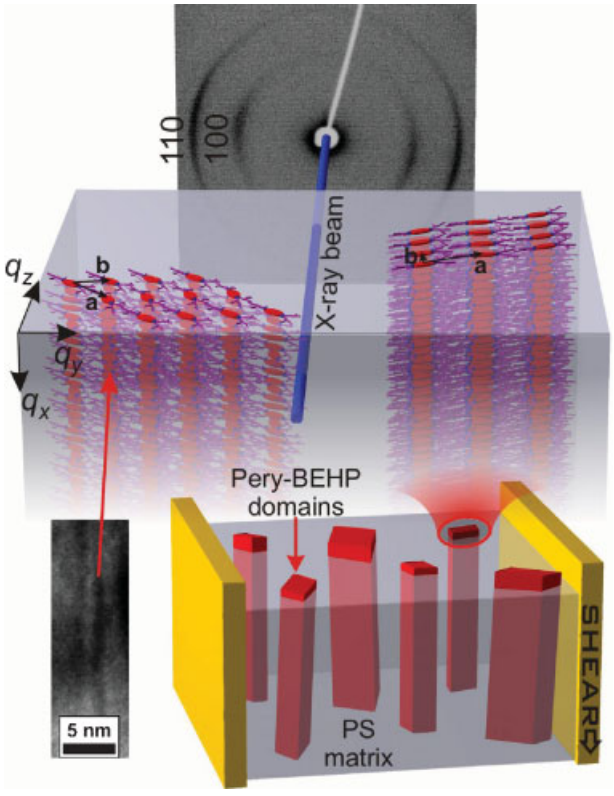

Figure 6. Schematic representation illustrating how the shear alignment in the proposed case works at different length scales. At the mesoscale the entangled matrix polymer chains align the elongated columnar liquid-crystalline Pery-BEHP aggregates due to the flow field. The columnar liquid-crystalline aggregates, in turn, have well-defined internal columnar order, which leads to alignment of the optically active perylenes on a molecular level. The flow direction is along the aggregates.

2.4. Structure of the Shear Aligned Pery-BEHP/PS Blend

Combining the structural and optical studies, one can now propose a structure for the shear-aligned Pery-BEHP/PS blends (Fig. 6). Macroscopic phase separation between Pery-BEHP and PS after shear is excluded by the Maltese cross type structure observed in polarized optical microscopy (Fig. 7b). On the other hand, complete miscibility between Pery-BEHP and PS is also excluded, as SAXS shows the same periodicity for Pery-BEHP in blends as for the case of the pure Pery-BEHP complex (Figs. 1 and 3). Therefore, Pery-BEHP must be present as dispersed aggregates of self-assembled columnar liquid crystals within the PS matrix. Importantly, the above reasoning and results show that at least some of the dimensions of the dispersed Pery-BEHP aggregates must be smaller than macroscopic length scale, i.e., they have to be mesoscale. There the alkyl surface activity of Pery-BEHP may be important. In fact, careful TEM investigation proved the existence of such aggregates: extended objects were observed within the Pery-BEHP/PS blends with internal periodic structure which is exactly the same as observed in the bulk Pery-BEHP complexes (Fig. 6). More quantitatively, an estimate for the lateral size of the Pery-BEHP aggregates with the PS-matrix can be obtained in the following way: analysis of the peak width of the 110 reflection in the scattering pattern of the aligned Pery-BEHP/PS4 blend (see Fig. 3f) in conjunction with a silver behenate standard and employing the Scherrer equation[46] yields the average assembly size (see Eq. 3 in the Experimental part). This analysis yields a value of $L = 450$ Å for the average lateral dimension of the Pery-BEHP aggregates in this particular case. We strongly emphasize, that the size and the shape of such domains are expected to depend on the processing conditions. The extended persistent shape observed in TEM is most probably stabilized by the strong stacking interactions in the extended columnar structure. This extended shape is essential to allow efficient alignment using the shear flow field provided by the entangled matrix polymer chains. The alignment, in turn, leads to preferred orientation of the perylenes due to existence of structures at different length

scales and thus to the observed optical and scattering properties.

Therefore, we suggest that the feasibility of the observed shear alignment depends on several length scales: the extended LC aggregates couple well with the shear alignment within the high MW matrix with entanglements, and the columnar LC aggregates exhibit shape persistence which allows for alignment of individual perylene moieties within the aggregates.

3. Conclusions

In conclusion, the present study deals with a fundamental problem of ionic self-assembled nanostructures: in spite of their promise as modular materials for, e.g., optical and electrical applications, their overall alignment has remained a challenge, in particular when aiming at a technically feasible and straightforward process. Taking perylene as an important optically active material, here we first show that the ionic self-assembled *N*,*N*′-bis(ethylenetrimethylammonium)perylenediimide/bis(2-ethylhexyl) phosphate complex (Pery-BEHP) forms columnar liquid crystals in bulk. Such perylene-surfactant complexes cannot be aligned by shear or any other methods so far identified, thus limiting their use for optical applications. Blending Pery-BEHP with PS leads to high aspect ratio aggregates with mesoscale lateral dimensions, showing internal columnar LC order. Selecting PS with sufficiently high MW, shearing leads to efficient alignment of the elongated LC aggregates at the mesoscale. As the LC aggregates, in turn, have well-defined internal self-assembled order, the shearing leads to high alignment of the perylenes on the molecular scale, with macroscopic optical properties. Therefore, rather than trying to order the perylene molecules directly, we shear align extended liquid-crystalline aggregates which couple better with the flow fields. We suggest that this approach for ordering using several length scales can be generalized to several other imposed external fields, even electric fields, and could have impact on the areas of optical, electronic, porous materials, and facile preparation of macroscopically aligned electroactive nanocomposites.

4. Experimental

Materials: *N*,*N*′-bis(2-(trimethylammonium)ethylene)-perylene-3,4,9,10-tetra-carboxyldiimide-bis(ethyl-hexyl)phosphate, (Pery-BEHP) was synthesized according to the procedure reported in references [21,22]. Six different homopolymers of polystyrene (PS) were obtained from Polymer Source and they were used as received. All polymers including their molecular weight and polydispersity are listed in Table 1. To prepare blends of Pery-BEHP complex in PS both the complex and the PS were separately dissolved in analytical grade chloroform and, after stirring, were mixed to yield solutions with 5 wt % concentration of Pery-BEHP within the total Pery-BEHP/PS composition. Chloroform was then slowly evaporated, where after the samples were dried under vacuum at 30 °C for at least 2 days.

Instrumentation: Small-angle X-ray scattering (SAXS) measurements were performed using a Bruker SAXS system ($U = 45$ kV, $I = 60$ mA, $\lambda = 1.54$ Å) including a 2D area detector (Bruker AXS). The sample to detector distance was approximately 44 cm. The magnitude of the scattering vector is given by $q = (4\pi/\lambda)\ \sin\theta$, where 2θ is the scattering angle and the q-range was calibrated using a silver behenate standard. The average aggregate size of Pery-BEHP in the PS matrix was estimated by using the Scherrer equation [46] to determine the average thickness of the crystals according to

$$L = \frac{0.9\lambda}{\Delta(2\theta)\cos\theta} \quad (3)$$

where $\lambda = 1.54$ Å is the wavelength of the X-ray radiation and $\Delta(2\theta)$ is the full width at half-maximum (FWHM) for the corresponding diffraction peak at the scattering angle 2θ. Instrumental broadening was taken into account by using silver behenate as a standard (typical crystallite size [47] $L = (900 \pm 50)$ Å) and assuming Gaussian peak shape for both the 110 peak of Pery-BEHP/PS and the 001 peak of the standard. Wide-angle X-ray scattering measurements (WAXS) were done using a Nonius PDS120 powder diffractometer in transmission geometry including a FR590 generator. A Nonius CPS120 position sensitive detector (resolution in 2θ is 0.018 °) was used to measure the scattered radiation. For transmission electron microscopy (TEM) Pery-BEHP sample was embedded in epoxy and cured at room temperature, followed by microtoming with a Leica Ultracut UCT-ultramicrotome and a Diatome diamond knife to yield sections of approximately 40 nm in thickness. For the aligned Pery-BEHP/PS4 samples a similar sample preparation method was used, except that sections were cut directly from the aligned pellet without embedding in epoxy. The sections were imaged in bright field using a FEI Tecnai 12 transmission electron microscope operating at an acceleration voltage of 120 kV. Rheological measurements and shear alignment were performed on a Bohlin CS-50 stress controlled rheometer equipped with 10 mm diameter plate/plate geometry and a custom-made oven. The sample material was first pressed into a pellet and thereafter placed between the plates of the rheometer, heated to the measurement temperature and allowed to equilibrate for 15 minutes. Ultraviolet-visible (UV-Vis) spectra of the aligned samples were collected using a Perkin-Elmer Lambda 950 spectrometer. This setup included a depolarizer/polarizer drive that was used to record spectra at two different angles, namely polarization of the incident light being parallel and perpendicular to the shearing direction. Absorbancies at these angles yield the dichroic ratio according to $D(\lambda) = A_{\perp}(\lambda)/A_{||}(\lambda)$ where $A_{\perp}(\lambda)$ is the absorbance in the perpendicular and $A_{||}(\lambda)$ in the parallel direction. Photomicrographs were taken with a Nikon Type 104 optical microscope equipped with crossed polarizers.

Received: December 20, 2007
Revised: February 19, 2008

[1] G. M. Whitesides, B. Grzybowski, *Science* **2002**, *295*, 2418.
[2] M. Muthukumar, C. K. Ober, E. L. Thomas, *Science* **1997**, *277*, 1225.
[3] H. Engelkamp, S. Middelbeek, R. J. M. Nolte, *Science* **1999**, *284*, 785.
[4] V. Percec, M. Glodde, T. K. Bera, Y. Miura, I. Shiyanovskaya, K. D. Singer, V. S. K. Balagurusamy, P. A. Heiney, I. Schnell, A. Rapp, H. W. Spiess, S. D. Hudson, H. Duan, *Nature* **2002**, *419*, 384.
[5] C. F. J. Faul, M. Antonietti, *Adv. Mater.* **2003**, *15*, 673.
[6] O. Ikkala, G. ten Brinke, *Chem. Commun.* **2004**, 2131.
[7] F. J. M. Hoeben, P. Jonkheijm, E. W. Meijer, A. Schenning, *Chem. Rev.* **2005**, *105*, 1491.
[8] T. Kato, N. Mizoshita, K. Kishimoto, *Angew. Chem. Int. Ed.* **2006**, *45*, 38.

[9] Z. R. Chen, J. A. Kornfield, S. D. Smith, J. T. Grothaus, M. M. Satkowski, *Science* **1997**, *277*, 1248.
[10] J. Sanger, W. Gronski, H. Leist, U. Wiesner, *Macromolecules* **1997**, *30*, 7621.
[11] R. Makinen, J. Ruokolainen, O. Ikkala, K. de Moel, G. ten Brinke, W. De Odorico, M. Stamm, *Macromolecules* **2000**, *33*, 3441.
[12] T. Thurn-Albrecht, J. Schotter, C. A. Kastle, N. Emley, T. Shibauchi, L. Krusin-Elbaum, K. Guarini, C. T. Black, M. T. Tuominen, T. P. Russell, *Science* **2000**, *290*, 2126.
[13] A. Boker, A. Knoll, H. Elbs, V. Abetz, A. H. E. Muller, G. Krausch, *Macromolecules* **2002**, *35*, 1319.
[14] T. Ruotsalainen, M. Torkkeli, R. Serimaa, T. Makela, R. Maki-Ontto, J. Ruokolainen, G. ten Brinke, O. Ikkala, *Macromolecules* **2003**, *36*, 9437.
[15] J. Hoogboom, T. Rasing, A. E. Rowan, R. J. M. Nolte, *J. Mater. Chem.* **2006**, *16*, 1305.
[16] Y. Zakrevskyy, J. Stumpe, C. F. J. Faul, *Adv. Mater.* **2006**, *18*, 2133.
[17] A. F. Thunemann, *Prog. Polym. Sci.* **2002**, *27*, 1473.
[18] S. Bondzic, J. de Wit, E. Polushkin, A. J. Schouten, G. ten Brinke, J. Ruokolainen, O. Ikkala, I. Dolbnya, W. Bras, *Macromolecules* **2004**, *37*, 9517.
[19] G. A. van Ekenstein, E. Polushkin, H. Nijland, O. Ikkala, G. ten Brinke, *Macromolecules* **2003**, *36*, 3684.
[20] F. Wurthner, *Chem. Commun.* **2004**, 1564.
[21] Y. Guan, Y. Zakrevskyy, J. Stumpe, M. Antonietti, C. F. J. Faul, *Chem. Commun.* **2003**, 894.
[22] Y. Zakrevskyy, C. F. J. Faul, Y. Guan, J. Stumpe, *Adv. Funct. Mater.* **2004**, *14*, 835.
[23] E. Polushkin, A. Laiho, G. A. van Ekenstein, D. Franke, O. Ikkala, G. ten Brinke, C. F. J. Faul, unpublished.
[24] Y. Zakrevskyy, J. Stumpe, B. Smarsly, C. F. J. Faul, *Phys. Rev. E.* **2007**, *75*, 031703.
[25] L. Schmidt-Mende, A. Fechtenkotter, K. Müllen, E. Moons, R. H. Friend, J. D. MacKenzie, *Science* **2001**, *293*, 1119.
[26] F. Wurthner, Z. J. Chen, F. J. M. Hoeben, P. Osswald, C. C. You, P. Jonkheijm, J. von Herrikhuyzen, A. Schenning, P. van der Schoot, E. W. Meijer, E. H. A. Beckers, S. C. J. Meskers, R. A. J. Janssen, *J. Am. Chem. Soc.* **2004**, *126*, 10611.
[27] F. Wurthner, C. Thalacker, S. Diele, C. Tschierske, *Chem. Eur. J.* **2001**, *7*, 2245.
[28] M. Okamoto, P. H. Nam, P. Maiti, T. Kotaka, N. Hasegawa, A. Usuki, *Nano Lett.* **2001**, *1*, 295.
[29] P. M. Ajayan, O. Stephan, C. Colliex, D. Trauth, *Science* **1994**, *265*, 1212.
[30] J. Yonezawa, S. M. Martin, C. W. Macosko, M. D. Ward, *Macromolecules* **2004**, *37*, 6424.
[31] C. Y. Yang, Y. Cao, P. Smith, A. J. Heeger, *Synth. Met.* **1993**, *53*, 293.
[32] M. S. Kim, K. Levon, *J. Colloid Interface Sci.* **1997**, *190*, 17.
[33] A. Pud, N. Ogurtsov, A. Korzhenko, G. Shapoval, *Prog. Polym. Sci.* **2003**, *28*, 1701.
[34] A. Fizazi, J. Moulton, K. Pakbaz, S. Rughooputh, P. Smith, A. J. Heeger, *Phys. Rev. Lett.* **1990**, *64*, 2180.
[35] S. Goffri, C. Muller, N. Stingelin-Stutzmann, D. W. Breiby, C. P. Radano, J. W. Andreasen, R. Thompson, R. A. J. Janssen, M. M. Nielsen, P. Smith, H. Sirringhaus, *Nat. Mater.* **2006**, *5*, 950.
[36] U. Beginn, G. Zipp, A. Mourran, P. Walther, M. Moller, *Adv. Mater.* **2000**, *12*, 513.
[37] J. Z. Jin, V. Nguyen, W. Q. Gu, X. Y. Lu, B. J. Elliott, D. L. Gin, *Chem. Mater.* **2005**, *17*, 224.
[38] E. R. Zubarev, M. U. Pralle, E. D. Sone, S. I. Stupp, *J. Am. Chem. Soc.* **2001**, *123*, 4105.
[39] E. R. Zubarev, M. U. Pralle, E. D. Sone, S. I. Stupp, *Adv. Mater.* **2002**, *14*, 198.
[40] J. C. Stendahl, L. M. Li, E. R. Zubarev, Y. R. Chen, S. I. Stupp, *Adv. Mater.* **2002**, *14*, 1540.
[41] The interpretation of the scattering data is based on the assumption that the structure is homogeneous, which means that all the SAXS peaks correspond to one structure and not a mixture. However, the presence of a mixture can be excluded based on the SAXS data. First of all the SAXS pattern was reproducible, which is usually not the case for ill-defined mixtures and secondly the ratios between the peak positions are such that it is almost impossible to find two sets of SAXS peaks belonging to two simpler structures (e.g, lamellar, 2D hexagonal).
[42] S. H. Wu, *Polym. Eng. Sci.* **1987**, *27*, 335.
[43] G. M. Jordhamo, J. A. Manson, L. H. Sperling, *Polym. Eng. Sci.* **1986**, *26*, 517.
[44] P. H. Hermans, *Contribution to the Physics of Cellulose Fibres*, Elsevier, Amsterdam **1946**.
[45] L. J. Fetters, D. J. Lohse, D. Richter, T. A. Witten, A. Zirkel, *Macromolecules* **1994**, *27*, 4639.
[46] A. Guinier, *X-ray Diffraction in Crystals, Imperfect Crystals, and Amorphous Bodies*, Dover, Publications, New York **1994**.
[47] T. C. Huang, H. Toraya, T. N. Blanton, Y. Wu, *J. Appl. Crystallogr.* **1993**, *26*, 180.